

A Riemann Manifold Model Framework for Longitudinal Changes in Physical Activity Patterns

Jingjing Zou * ¹, Tuo Lin¹, Chongzhi Di², John Bellettiere¹, Marta M. Jankowska³, Sheri J. Hartman^{1,6}, Dorothy D. Sears^{4,5,6}, Andrea Z. LaCroix¹, Cheryl L. Rock⁵, and Loki Natarajan ^{1,6}

¹Herbert Wertheim School of Public Health and Human Longevity Science, University of California, San Diego

²Division of Public Health Sciences, Fred Hutchinson Cancer Research Center

³Department of Population Sciences, Beckman Research Institute, City of Hope

⁴College of Health Solutions, Arizona State University; Department of Family Medicine, University of California, San Diego

⁵Department of Family Medicine, School of Medicine, University of California, San Diego

⁶UC San Diego Moores Cancer Center

February 8, 2022

Abstract

Physical activity (PA) is significantly associated with many health outcomes. The wide usage of wearable accelerometer-based activity trackers in recent years has provided a unique opportunity for in-depth research on PA and its relations with health outcomes and interventions. Past analysis of activity tracker data relies heavily on aggregating minute-level PA records into day-level summary statistics, in which important information of diurnal PA patterns is lost. In this paper we propose a novel functional data analysis approach based on theory of Riemann manifolds for modeling PA records and longitudinal changes in PA temporal patterns. We model smoothed minute-level PA of a day as one-dimensional Riemann manifolds and longitudinal changes in PA in different visits as deformations between manifolds. A key quantity of the deformations are the “initial momenta”, which are vector fields representing directions and magnitudes to “drag” each point on a baseline PA curve towards a follow-up visit curve. The variability in changes of PA among a cohort of subjects is characterized via variability in the deformation momenta. Functional principal components (PC) analysis is further adopted to model deformation momenta and PC scores are used as a proxy in modeling the relation between changes in PA and health outcomes and/or interventions. With the proposed approach, we conduct comprehensive analyses on data from two clinical trials: Reach for Health (RfH) and Metabolism, Exercise and Nutrition at UCSD (MENU),

*DDS (Dody), SH, CLR (Cheryl), MJ and LN were partially supported by funding from the National Cancer Institute (U54 CA155435-01); JB, AC, MJ, JZ, and LN were partially supported by funding from the National Institute of Diabetes and Digestive and Kidney Disease (R01DK114945); JB, AC, CD, DDS, SH, and LN were partially supported by funding from the National Institute of Aging (PO1AG052352)

focusing on the effect of interventions on longitudinal changes in PA patterns and how different patterns of changes in PA influence weight loss, respectively. For both studies, important modes of variation in PA were identified to be significantly associated with lifestyle interventions/health outcomes. The proposed model and methods open up a new direction for statistical inference on longitudinal changes in PA.

Keywords: Activity trackers, accelerometer, functional data analysis, Riemann manifold, longitudinal analysis, functional principal component analysis

1 Introduction

Physical activity (PA) has been linked to health in many epidemiological studies. Physical inactivity and sedentary behavior are known risk factors for cardiovascular disease, cancer and all-cause mortality (Bijnen et al. (1994); Kohl (2001); Knoop et al. (2004); Sullivan et al. (2005); Blair (2009); Khan and Scott (2009); Wilmot et al. (2012); LaMonte et al. (2018); LaCroix et al. (2019); Chastin et al. (2019); Bellettiere et al. (2020); Parada et al. (2020)).

Activity trackers based on sensor devices such as accelerometers enables detailed tracking of daily PA at minute-level in free-living environment. In studies using activity trackers, participating subjects wear the device in body parts such as hip, thigh or wrist, and perform their usual daily activities non-intrusively (Prince et al. (2008); Colley et al. (2011); Dyrstad et al. (2014); Adamo et al. (2009); Ainsworth et al. (2014)). For systematic reviews and meta-analyses on data from accelerometer-based trackers, see Migueles et al. (2017); Stamatakis et al. (2019); Ekelund et al. (2019).

The emerging usage of activity trackers in studies provides an unprecedented opportunity for in-depth research on physical activity and sedentary behavior. In particular, recording PA of subjects with activity trackers in multiple visit periods, including the baseline and follow-ups, not only reveals information on PA during each period, but also enables estimation of longitudinal changes in PA between periods different visits. As a result, the impact of interventions, if incorporated in the study, can be evaluated by examining

the association between the intervention and longitudinal changes in PA. Moreover, the effect of longitudinal changes in PA on health outcomes such as obesity and physiological measurements relevant to diseases can be studied in correlative analysis of changes in PA and outcomes of interest.

The aforementioned analyses require statistical modeling of PA with minute-level activity tracker data and of the longitudinal changes in PA. Past studies of activity tracker data rely heavily on summarizing statistics, which aggregate minute-level data into single day-level measurements such as assessed sedentary time (SED), light-intensity physical activity (LIPA), and moderate-to-vigorous physical activity (MVPA) (Nader et al. (2008); Matthews et al. (2002); Loprinzi (2016); Füzéki et al. (2017)).

Each of the day-level measurements summarizes a facet of the activity tracker data. However, important information contained in the minute-level records can be lost in the process of extracting day-level measurements. In particular, the temporal dependence in activity levels at different times of a day cannot be assessed after day-level reduction of data complexity. As a result, the diurnal patterns of daily PA of each subject and the variability in the PA patterns cannot be included in the scope of the studies.

In more recent studies, functional data analysis (FDA) approaches that preserve the original format of the minute-level data instead of aggregating them into summary statistics have been adopted in explaining variability in PA, especially in temporal activity patterns, among subjects within one cohort. Instead of summarizing the minute-level activity tracker data using day-level measurements, FDA approaches treat the minute-level activity in a day as one single object and model PA records as a function of time of a day. The parameter of interest is temporal patterns of PA.

In these studies, the activity level recorded throughout the active hours of a day is usually characterized as a subject-specific $X_{ij}(t)$ indexed by chronological time t , where i and j index subjects and visits respectively. Variability in PA is usually modeled with

functional principal component analysis (fPCA) type of variance decomposition method. For example, Li et al. (2014) modeled jointly the energy expenditure and interruptions to sedentary behaviors with fPCA. Goldsmith et al. (2015) proposed a generalized multilevel fPCA model to study minute-level PA recorded by activity trackers of subjects in multiple days. The variability in PA was decomposed into subject-level and day-level nested random effects after residualizing over relevant fixed effect covariates. The model parameters were then estimated using Bayesian methods. Li et al. (2015) extended the model in Goldsmith et al. (2015) and proposed a three-level functional data model allowing daily records to be nested in weeks. The model parameters were estimated with extended expectation/conditional maximization either (ECME) algorithm. For details of multilevel fPCA and its applications to longitudinal functional data, see, for example, Di et al. (2009) and Greven et al. (2010, 2011).

Studies focusing on other aspects of PA records have also been conducted. Xiao et al. (2015) proposed a covariate-dependent functional model to quantify the lifetime circadian rhythm of PA. Shou et al. (2014) discussed a structured functional principal component analysis method to handle multiple levels of variation generated by nested and crossed study designs. Goldsmith et al. (2016) adopted function-on-scalar regression methods to relate 24-hour diurnal PA patterns with covariates. Xu et al. (2019) implemented a fPCA mixed model to study multiple daily PA records measured by the activity tracker and examined the association between activity patterns and health outcomes. Reuter et al. (2020) proposed a two-stage clustering method for sedentary behavior (SB) and examined associations between SB patterns and longitudinal physical functioning with a mixed model.

Despite the recent development of FDA approaches for minute-level PA data, it remains unclear how to directly model longitudinal changes in PA of subjects in a cohort while treating PC records in each period as functional objects and thus the need of new statistical models and methods. Moreover, statistical models are needed for examining relationship

between the longitudinal changes in PA and health outcomes and interventions.

Directly modeling the changes in PA will also enable visualizing and interpreting modes of the longitudinal changes in PA, which is especially important in understanding the relationship between changes in PA and interventions as well as effects of different modes of variation in PA on health outcomes. For example, enhanced activity in certain time windows and/or shifts of active hours to certain periods can be associated with interventions and/or health outcomes of interest (Khan et al. (2021)). This type of information can be valuable in patient consultation and in designing individualized intervention programs according to a patient’s personal medical history and conditions.

In this paper we propose a new model framework for studying longitudinal changes in PA and relations between the longitudinal changes in activity and health outcomes and/or interventions. The model framework consists of multiple stages. First, we model activity-tracker-recorded PA using a Riemann manifold framework, in which pre-processed and smoothed minute-level PA records are characterized as one-dimensional (1D) Riemann manifolds (curves). Next, the longitudinal changes in PA as reflected by activity tracker records at baseline and follow-up visit periods are modeled as deformations between PA curves obtained from consecutive visits. Specifically, the deformations are modeled by diffeomorphisms governed by elements in a reproducing kernel Hilbert space that satisfy minimal-energy constraints. A key quantity in modeling the deformations are the “initial momenta”, which are vector fields that represent the initial directions and magnitudes to “drag” each point on the baseline curve towards the target curve and determine the deformation from one curve to another (Beg et al. (2005); Vaillant et al. (2004)). Results on diffeomorphisms have been used in matching and registration of medical images such as structural brain fMRI, see, for example, Hernandez et al. (2009). However, to our best knowledge, this is one of the first studies of longitudinal changes in physical activity utilizing the power of diffeomorphism theory. In estimating the model parameters in the

diffeomorphisms of Riemann manifolds, we use methods and algorithms in the Matlab package “fshapesTK” by Charlier et al. (2015a).

Modeling longitudinal changes in PA as deformations between PA curves is a functional data analysis (FDA) approach. Instead of treating PA at different time points separately, the proposed approach preserves intrinsic diurnal patterns of PA as functions of time of a day. Moreover, the deformations are estimated with a constraint of minimized energy, enabling a smooth transition of PA at adjacent time points.

Comparing to existing approaches, an important advantage of modeling the longitudinal changes in PA as deformations between PA curves is that it allows not only modeling of vertical changes of PA magnitude at each fixed time point of a day in different visit periods (as given by merely taking the difference in PA between visits), but also potential temporal shifts of diurnal activity patterns. The capability of capturing phase changes is especially important in the study of PA, as subjects can experience change of circadian rhythms and habits and may exhibit a shift of active hours (Montaruli et al. (2017)). With the proposed model and methods, researchers will be able to identify changes in both magnitude and phase via directions and magnitudes of estimated deformation momenta. Detailed discussion and demonstration of the capability of the proposed approach in this regard are provided in the example of Figure 5 in later sections.

We further model the variability in longitudinal changes of PA with functional PCA to reduce the dimensionality of the statistics used to characterize the deformations. Principal components (PC) that are capable of explaining a majority of the variability are adopted as the main modes of longitudinal changes in PA, and the corresponding projection coefficients (scores) on the PCs for each subject are used to characterize the composition of different modes of variation in subject-specific PA changes.

Finally, the relations between longitudinal changes in PA and health outcomes and/or interventions are modeled via the relations between subject-specific PC projection coefficients

and health outcomes and/or interventions.

The model and method proposed here are applied to data from two large scale longitudinal clinical trials: the Reach for Health (RfH) and Metabolism, Exercise and Nutrition at UCSD (MENU) study. Both studies include minute-level activity records measured by activity trackers in multiple visiting periods. In line with the different designs and goals of the two studies, for the RfH data we focus on analyzing the effect of a lifestyle intervention on changes in PA, while for the MENU data we focus on analyzing the effects of different modes of variation in PA on health outcomes. For both datasets important modes of variation in PA are discovered and results are found to be intuitive and interpretable.

The paper is organized as follows. Section 2 introduces the backgrounds and data of the two studies that motivate the development of the proposed models and methods. Section 3 focuses on the formulation of the proposed Riemann manifold model framework for longitudinal changes in PA. Section 4 explains details of the estimation pipeline for parameters in the proposed model. Sections 6 and 7 examine the data from RfH and MENU studies under the proposed model framework, estimate model parameters and provide comprehensive interpretations of the results.

2 Data Motivation

The model and method proposed in this paper are motivated by two clinical trials: Reach for Health and Metabolism, Exercise and Nutrition at UCSD (MENU). Both studies were part of the NIH-funded Transdisciplinary Research on Energetics and Cancer (TREC) Study at University of California, San Diego (UCSD) from 2011 to 2017. The goal of the studies was to gain a deeper understanding of the influence of obesity and energetics on cancer risk (Xu et al. (2019)).

The RfH study is a six-month clinical trial that involved 333 overweight, postmenopausal

early-stage breast cancer survivors in a 2×2 randomized design. Each of the subjects was randomly assigned to either metformin treatment or placebo, combined with either a lifestyle-based intervention or placebo. The primary aim was to test the effect of treatments on health outcomes, especially weight loss as measured by the change in BMI (Patterson et al. (2018)).

The MENU study is a 12-month behavioral intervention study on 245 overweight and otherwise healthy women. Each subject was randomly assigned to one of the three diet treatment groups: lower fat and higher carbohydrate, lower carbohydrate and higher monounsaturated fat, and walnut-rich and lower carbohydrate (Rock et al. (2016); Le et al. (2016); Patterson et al. (2016)). The goal was to study the role of dietary macronutrient composition by examining the effects of the treatments on weight loss. Data were collected in a similar procedure in both trials. Demographic information, lifestyle and health-related measurements were collected at baseline. If changes were of interest, measurements were also collected at follow-up visits.

In addition, for both studies, each subject's daily PA at baseline and follow-up periods were measured by the GT3X ActiGraph (ActiGraph, LLC; Pensacola, FL; www.actigraphcorp.com), a research-grade activity tracker with built-in triaxial accelerometer. Participants were told to wear the ActiGraph on the right hip during all their waking hours for seven consecutive days about one week before their visits at baseline and follow-ups. The accelerometers of ActiGraph were set up to collect high-resolution activity data at 30 Hz, which were then processed into minute-level tri-axial counts data by the Actilife software. Total activity magnitudes per minute were obtained by aggregating magnitudes of three dimensions (Xu et al. (2019); Bassett (2012)). See the Supp. Material for an example of a subject's PA record in one day.

3 The Model Framework

3.1 A Riemann Manifold Model for Physical Activity

Suppose there are N subjects in the study. For the i th subject, daily physical activity (PA) is recorded by the activity tracker in periods $k = 0, \dots, K$, where $k = 0$ denotes the baseline visit and $k = 1, \dots, K$ denote the follow-ups. Data of each period consist of daily minute-level PA records of several consecutive days. The multi-day PA records in each period are averaged along chronological time t of a day and smoothed to reduce noise (details are explained in Section 4). The resulting average PA at different times $t \in [0, T]$ of a day are represented by one-dimensional Riemann manifolds (curves) $X_i^{(k)}$ with images on $E = [0, T] \times [0, M] \subset \mathbb{R}^2$, where M denotes the maximal admissible PA magnitude.

Longitudinal changes in PA between visits are modeled via diffeomorphisms that deforms a subject's PA curve at one visit to that of another. Let $C_0^1(E, E)$ denote the space of continuous differentiable functions from E to itself, and let V be the reproducing kernel Hilbert space (RKHS) of vector fields embedded in $C_0^1(E, E)$. Consider the space $L^2([0, 1], V)$ in which each element $v : [0, 1] \rightarrow V$ is a set of time-varying vector fields indexed by $\tau \in [0, 1]$ and has finite L^2 norm: $\int_0^1 \|v_\tau\|^2 d\tau < \infty$. Note τ should not be mixed up with the chronological time t in a day.

Let G_V denote the group of diffeomorphisms obtained by *flowing* vector fields in $v \in L^2([0, 1], V)$ (Charlier et al. (2015b)). Each element $\phi \in G_V$ satisfies $\phi(v, \cdot) = \psi_v(1, \cdot)$, where ψ_v is the solution to the ordinary differential equations (ODE) governed by the vector fields v_τ :

$$\frac{\partial}{\partial \tau} \psi_v(\tau, \cdot) = v_\tau \circ \psi_v(\tau, \cdot) \quad (1)$$

that satisfies the initial condition $\psi_v(0, \cdot) = \text{Id}$ which denotes the identity mapping on E .

The variability of the longitudinal changes in PA among subjects in the cohort is characterized by the subject-specific random vector fields $\{v_i^{(k)} : i = 1, \dots, N, k = 1, \dots, K\}$

in which each $v_i^{(k)}$ is defined on $L^2([0, 1], V)$. For simplicity of notation we omit the time index τ in the subject-specific $v_i^{(k)}$ whenever there is no ambiguity. For each i and k , assume the longitudinal change in the PA from visit $(k - 1)$ to k satisfies

$$X_i^{(k)} = \phi(v_i^{(k)}, \cdot) \circ X_i^{(k-1)}, \quad (2)$$

in which $\phi(v_i^{(k)}, \cdot)$ is the diffeomorphism associated with the subject-specific vector field $v_i^{(k)}$.

The deformation $\phi_i^{(k)}(v_i^{(k)}, \cdot)$ that satisfies (2) is not unique. In fact, there are infinite numbers of deformations that can transform $X_i^{(k-1)}$ to $X_i^{(k)}$. Further constraints are needed to uniquely define the vector field $v_i^{(k)}$ and its associated deformation $\phi_i^{(k)}(v_i^{(k)}, \cdot)$. Here we adopt the constraint on the deformation energy

$$\int_0^1 \|v_\tau\|^2 d\tau, \quad (3)$$

which is always finite given $v_\tau \in L^2([0, 1], V)$.

For each i and k , we model the change in the k th subject's PA between the $(k - 1)$ th and the k th with the deformation $\phi_i^{(k)}(v_i^{(k)}, \cdot)$ that satisfies (2) whose associated v_τ minimizes the energy (3). In Charlier et al. (2015b) it is shown that v_τ that minimizes the energy is unique and is in fact determined by v_0 , that is, the vector field at $\tau = 0$.

We further assume the following RKHS representation for each $v_i^{(k)}$: for any $\tau \in [0, 1]$,

$$v_\tau(\cdot) = \sum_{j=1}^{n_g} K_V(\phi_v(\tau, c_j), \cdot) m_{j,\tau}, \quad (4)$$

where $\{c_j : j = 1, \dots, n_g\} \subset \mathbb{R}^2$ is a set of pre-selected control points, $K_V(x, y) = \exp(-\|x - y\|^2 / (2\sigma_V^2)) \mathbf{I}_2$ is the Gaussian isotropic kernel with a fixed rigidity parameter σ_V^2 , and $m_{j,\tau} \in \mathbb{R}^2$ is the momenta of the deformation in the j th control point at τ . Therefore at each τ ,

the v_τ defined in (4) is a weighted average of the momenta in the control points smoothed by the Gaussian kernel, which implies that the deformation can be fully characterized by the momenta at the control points.

3.2 Functional Principal Component Analysis (fPCA) for the Deformations

Given the model introduced in the previous section for longitudinal changes in PA for each subject, and representation (4) of the deformation momenta, the variability of longitudinal changes in PA among subjects in the cohort can be represented further by a function principal component model.

For simplicity, we first assume $K = 1$ so that there is only one follow-up after the initial (baseline) visit. The case of multiple follow-ups can be readily extended: an extra dimension can be introduced for the visits, so that the domain of the vector fields at each τ becomes $\{1, \dots, K\} \times E$, and for each $k = 1, \dots, K$, the sub-vector-field $v : \{k\} \times E \rightarrow E$ denotes the vector field governing the deformation from the PA curve at the $(k - 1)$ th visit to the k th visit.

As in the RKHS representation (4), the deformation between PA in the baseline and the follow-up visits of the i th subject is characterized by the momenta $\{(m_{1,\tau}^i, \dots, m_{n_g,\tau}^i), \tau \in [0, 1]\}$. In fact, as discussed in the previous section, subject to the constraint of minimal energy, the initial momenta $m^i := (m_{1,0}^i, \dots, m_{n_g,0}^i)$ fully determine the deformation, and thus each subject's deformations between PA curves at different visits can be characterized by the initial momenta alone.

Consider the principal component representation of the initial momenta $m^i = \sum_{l=1}^{\infty} a_{il} \mu_l$, where $\{\mu_l : l = 1, \dots, \infty\} \subset \mathbb{R}^{n_g \times 2}$ are the principal components (PC) and $a_{il} = \langle m^i, \mu_l \rangle$, where $\langle \cdot, \cdot \rangle$ denotes the Frobenius inner product on $\mathbb{R}^{n_g \times 2}$, is the projection coefficient (score) of m^i on the l th PC.

Assume the variability in the deformations of subjects in the cohort can be well explained

by a finite number N_{pc} of principal components, so that we can write approximately $m^i = \sum_{l=1}^{N_{pc}} a_{il} \mu_l$. In practice, the value of N_{pc} can be determined using criteria such as the proportion of variance explained by the top PCs.

3.3 Correlative study with health outcomes

There are two types of questions that are often of interest to researchers: 1. how does one's PA react to interventions designed for encouraging more active lifestyle, and 2. how do longitudinal changes in PA affect health outcomes. To address these two questions, we model the relation between changes in PA and intervention and the relation between changes in PA and health outcomes with regressions, in which the longitudinal changes in PA are modeled through the PC projection coefficients $\{a_{il}\}$. The model is $a_{il} = f(X_i, Z_i) + \epsilon_{il}$ for effect of intervention X_i and covariates Z_i on changes in PA, and $Y_i = f(a_{i1}, \dots, a_{iN_{pc}}, Z_i) + \epsilon_i$ for effects of changes in PA on health outcomes. In both models the ϵ are independent and identically distributed (iid) errors.

4 Estimation Methods

In this section we delineate the estimation procedure for model parameters in Section 3. We focus on two groups of parameters: the parameters in modeling the longitudinal changes in PA using the Riemann manifold framework and the parameters in representing the group-level variability of changes in PA with fPCA. Parameters in models in Section 3.3 can be estimated with standard methods for regression models.

4.1 Estimation of Diffeomorphisms and Initial Momenta

Here we focus on the estimation of the deformation vector fields v and its associated initial momenta m in the diffeomorphism model described in Section 3.1.

In practice, each subject's PA records are available to the researcher in the discrete

format. In each visit, there are usually several consecutive days of PA records, and for each day the PA records are recorded in every minute from the morning to the evening by the accelerometer of the activity tracker. Daily PA records in the same visiting period are usually further averaged to reduce the noise. Therefore, for the k th period, the PA record consists of a series of points $(t, y(t))$, which are pairs of minutes in the day and the corresponding magnitudes of PA averaged over different days in the same visit.

The averaged PA records in each visit are then smoothed using splines with function *smooth.spline()* in software R 4.0.3 to further reduce noise caused by minor fluctuations of the activity tracker that are irrelevant to meaningful movements. We choose the degree of freedom (trace of smoothing matrix) $df = 25$ in spline smoothing based on exploratory analysis of datasets from both RfH and MENU studies so that the smoothed PA records preserve visible diurnal PA patterns while reducing minor noise induced by the trackers. Note here we use the same degree of freedom in smoothing the RfH and MENU PA records, as both studies use the GT3X Actigraph activity tracker to measure subjects' PA, leading to comparable noise levels in PA records from the two studies. For a different study using other activity tracker devices, the researcher can conduct exploratory analysis of the data to determine the appropriate smoothing parameter.

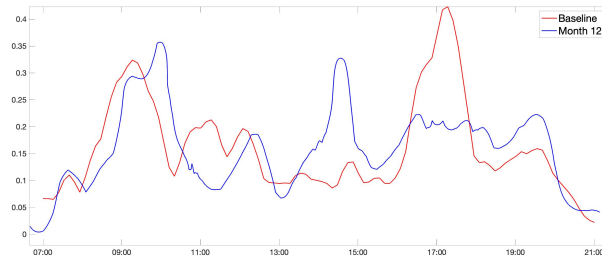


Figure 1: Example of PA curves at baseline and month-12 after smoothing, scaled by a common constant for all subjects.

The smoothed PA records can be treated approximately as curves: the series of $(t, y(t))$

after smoothing serve as the “skeleton” of the curve, and linear segments are used to connect PA records of consecutive minutes. For convenience we also scale all subject’s activity magnitudes by a common constant. The scaling is solely for simplicity in representation and will not affect the analysis results. As an example, Figure 1 displays the smoothed PA curves at baseline visiting period and month 12 from a subject in the MENU study.

For each subject i , we estimate the subject-specific deformation between smoothed PA curves $X_i^{(k-1)}$ and $X_i^{(k)}$ at the $k - 1$ th and k th visits respectively. The estimation of the deformation that transforms a subject’s PA curves from one (the *source* curve X_0) to another (the *target* curve X) is formulated as an optimization problem: the goal is to find the deformation that minimizes a dissimilarity metric g between the deformed source curve and the target curve, while constraining on the total energy $\int_0^1 \|v_\tau\|^2 d\tau$ of the deformation.

In computing the optimal deformation, the optimization problem with constraint on energy is transformed into an unconstrained problem with the following penalized objective function

$$\frac{\gamma_W}{2}g(\tilde{X}, X) + \frac{\gamma_V}{2} \int_0^1 \|v_\tau\|^2 d\tau, \quad (5)$$

where g is a dissimilarity metric based on Gaussian kernels between the observed target curve X and the estimated curve $\tilde{X} = \phi(v, \cdot) \circ X_0$, which is the result of deforming the source curve X_0 according to the vector field v . Here γ_V and γ_W are pre-selected penalty parameters for the energy and dissimilarity terms. For detailed format of the dissimilarity metric g , see Charlier et al. (2015b).

As discussed previously, the vector field v_τ is assumed to follow an RKHS representation

$$v(\cdot) = \sum_{j=1}^{n_g} K_V(\cdot, x_j) \cdot m_j, \quad (6)$$

where m_j are momenta on the k th control point on the curve. A natural choice of the control points are the time marks at which the activity tracker returns PA measurements.

To minimize the objective (5), it suffices to replace v with the expression (6) and minimize (5) over an admissible set of m_j with the Hamiltonian method in a backwards manner. The estimation algorithm “fsmatch_tan()” in Charlier et al. (2015b) is used for the estimation of the subject-specific optimal momenta. In particular, the initial momenta $\{\hat{m}_0^i : i = 1, \dots, N\}$ where $\hat{m}_0^i := (\hat{m}_{1,0}^i, \dots, \hat{m}_{n_g,0}^i)$ are estimated and serve as key quantities in the subsequent analysis.

4.2 fPCA of Momenta

The estimated initial momenta for the i th subject $\hat{m}_0^i := (\hat{m}_{1,0}^i, \dots, \hat{m}_{n_g,0}^i)$ is a vector field defined on the n_g landmark points and stored in an $n_g \times 2$ matrix. At each landmark point k , $\hat{m}_{k,0}^i$ is a two-dimensional vector indicating directions and magnitudes of the momenta in both the horizontal (x -axis) and vertical directions (y -axis). The momenta in the vertical direction indicates a change in PA level, while the momenta in the horizontal direction indicates a temporal shift of PA.

As described in Section 3.2, it is assumed that a finite number of functional principal components (PC) are adequate in explaining the majority of the variability in the deformation from the baseline to the month-12 PA curves for all subjects in a cohort. Calculating the PCs of dimension $\mathbb{R}^{n_g \times 2}$ under the Frobenius inner product is equivalent to calculating the PCs of vectors obtained from concatenating the \hat{m}^i matrices. The functional PCs and the corresponding subject-specific projection coefficients on the PCs can be estimated with the Matlab function `pca()` or equivalent algorithms in other statistical software.

To visualize the PCs, one can reshape the estimated initial momenta for each PC back to the original dimensionality $n_g \times 2$, and “flow” (as described in Section 3.1) a pre-selected template curve with the deformation governed by the estimated initial momenta. The resulting target curve can be used to interpret the modes of variations in PA associated with each PC.

In Sections 6 and 7, the proposed model and method are applied to the RfH and MENU datasets to explore the association between longitudinal PA change and health outcomes as well as interventions. The focus of the analysis for each dataset is different, however, given the different goals and study set-ups. For the RfH study, we are mainly interested in the association between the interventions and modes of changes in PA. For the MENU study, the focus is on the effect of different modes of changes in PA on health outcomes.

5 Simulation Studies

In this section we demonstrate the proposed estimation scheme with a synthetic dataset. The simulation studies consist of two stages: 1. the generation of baseline and follow-up PA curves of $N = 100$ subjects, and 2. the estimation of model parameters from the generated and observed PA curves.

First we generate a smooth baseline curve using the average baseline PA of the MENU study data, which consists of PA vector magnitudes (VM) at each of the 840 minutes from 7am to 9pm. Then we create 3 mutual-orthogonal principal components (PC), which are the initial momenta of three modes of changes in PA diurnal patterns from the baseline to the follow-up visit. As illustrated in Figure 2, the first PC is a general increase of PA levels throughout the day, the second is a local boost of PA, and the third is mainly a time shift of active hours to later times of the day. For details in generating the PCs, see the Supp. Material.

We generate each subject’s actual initial momenta of deformations as linear combinations of the initial momenta of the three PCs, where the coefficients in the linear combinations are simulated from independent Gaussian distributions with mean 0 and standard deviation 1, scaled by $(0.8, 1.2, 1.5)/2000$ for the coefficients of PC1, 2, and 3, respectively. Each of the 100 subject’s follow-up visit PA is generated by deforming the baseline PA curve following

the subject-specific initial momenta as described in Section 3.

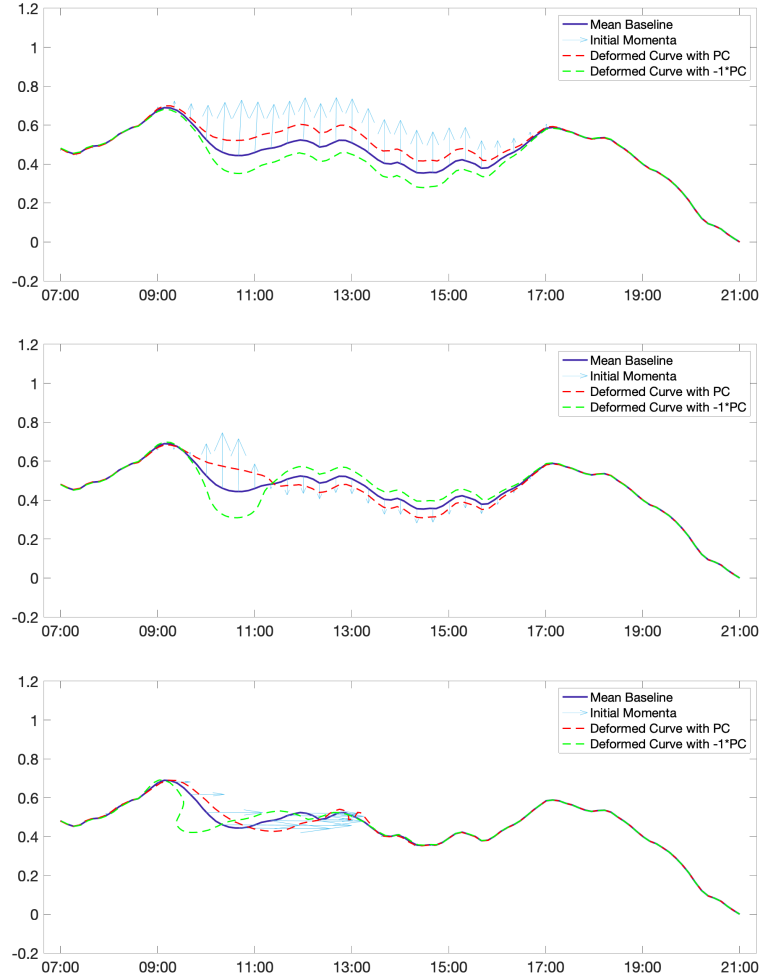


Figure 2: From top to bottom: actual initial momenta (blue arrows) of PC 1, 2, and 3 and deformations when applied to the baseline curve (solid navy) to deform into the follow-up curves (dashed red with PC and green with $-1 \times$ PC)

With the observed baseline and follow-up PA curves, we estimate the subject-specific initial momenta of the deformation with the proposed method. As a comparison, we also calculate the difference between the follow-up and baseline PA at each time point and extract PCs from the vertical differences. Figures 3 and 4 show the estimated PCs using the proposed method and the PCs extracted from vertical differences between the PA levels at baseline and the follow-up. It can be easily observed that the proposed method to a

large extend recovers the actual modes of longitudinal changes in PA by capturing most of the vertical changes in PA magnitudes and temporal shifts of local peaks. On the other hand, the PCA of vertical changes only between the baseline and follow-up PA levels is unsuccessful in displaying the major changes in PA diurnal patterns: the local increased PA of PC2 is recovered partially by the estimated PC1, but the overall increase of PA in the actual PC1 is not recovered with good accuracy, and the temporal shift of the actual PC3 is overlooked as expected.

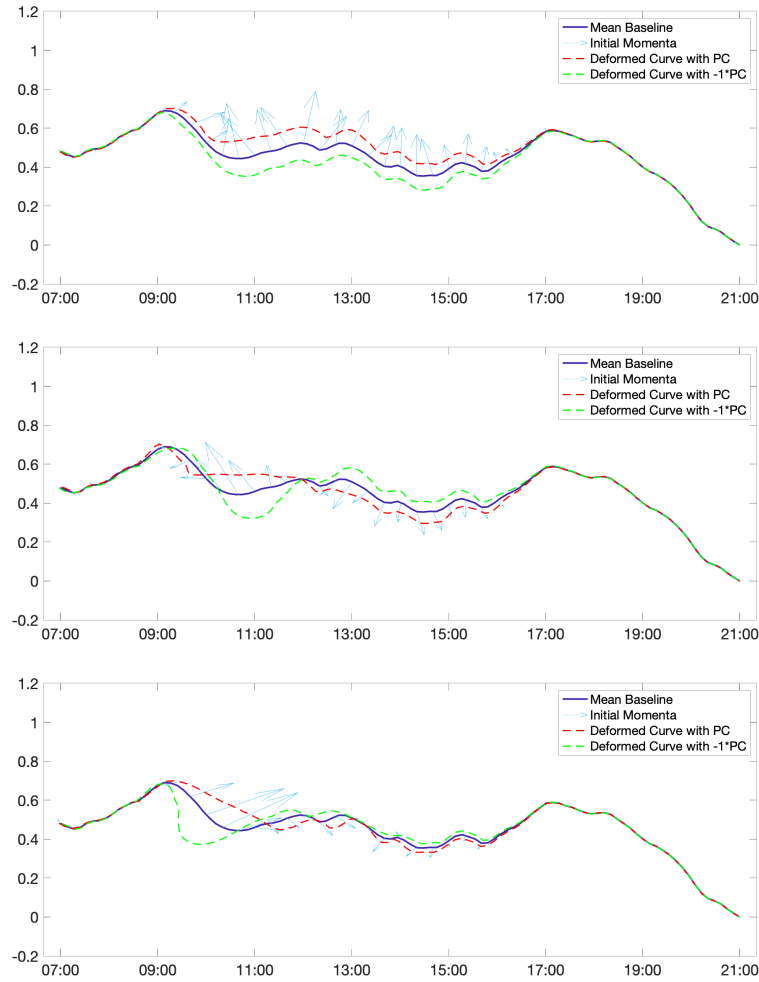


Figure 3: From top to bottom: estimated initial momenta with proposed approach (blue arrows) of PC 1, 2, and 3 and deformations when applied to the baseline curve (solid navy) to deform into the follow-up curves (dashed red with PC and green with $-1 \times$ PC)

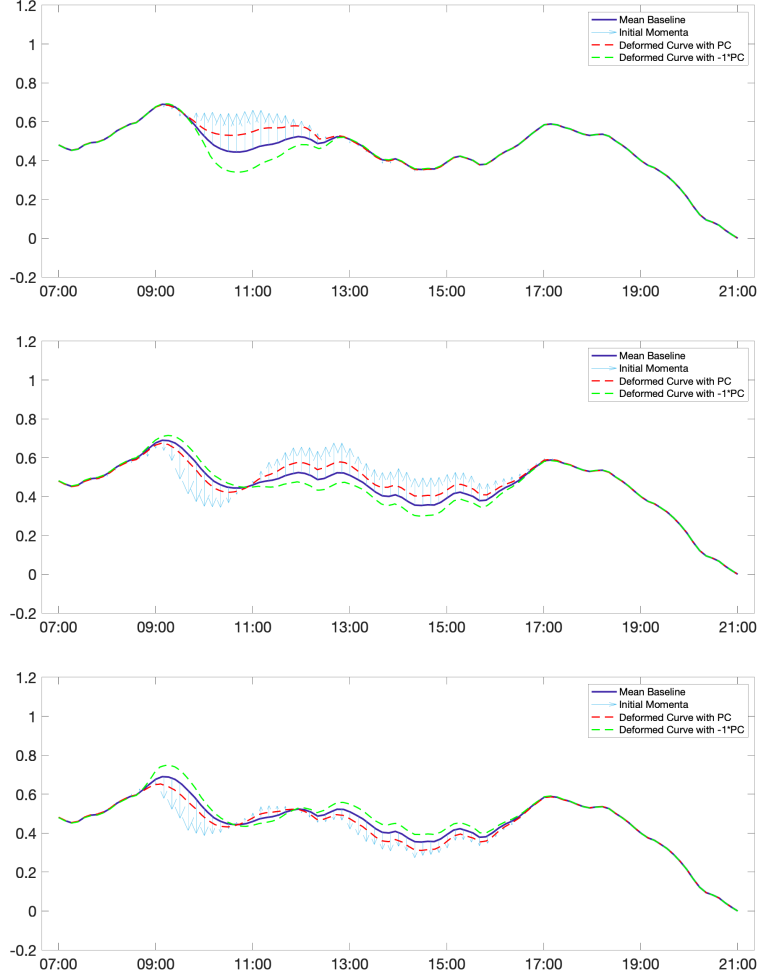


Figure 4: From top to bottom: estimated initial momenta with PCA applied to vertical differences between baseline and follow-up PA levels (blue arrows) of PC 1, 2, and 3 and deformations when applied to the baseline curve (solid navy) to deform into the follow-up curves (dashed red with PC and green with $-1 \times \text{PC}$)

6 Data Analysis I: the RfH Study

As introduced in Section 2, the RfH study data consist of PA records at baseline and month-6 for 333 overweight, postmenopausal early-stage breast cancer survivors. Each subject was randomly assigned to one of the 2×2 treatment arms. Our focus here is to study the effect of the treatments on the longitudinal changes in PA.

6.1 Pre-processing of Data

Subjects with both baseline and month-6 measurements available from the activity tracker are retained for the analysis. As a result, 303 out of 333 subjects remain in the dataset after cleaning for missing records.

For each subject, the baseline and month-6 activity tracker records are sorted by dates and time of wearing. We only use PA records of each day from 6am to midnight as most of the records out of this range can be omitted due to non-wear time when the subject was sleeping. Within the 6am-midnight window, whenever the subject was not wearing the device, PA was recorded as zero and treated as inactive time due to sleeping, since subjects were asked to wear the activity tracker during all waking hours except for time contacting water (Xu et al. (2019); Patterson et al. (2018)).

Note here we use the chronological time to index the PA records instead of align subjects' PA records according to the subject-specific time of first non-zero record, as of interest here are the diurnal activity patterns as a function of chronological time and the longitudinal change in such activity patterns.

The retained PA records for each subject are then averaged over the seven days within each visiting period. Consequently, for each subject averaged activity records indexed by time from 6am to midnight for the baseline and month-6 periods are available. We also scale all subject's activity magnitudes by a common constant. The scaling is solely for simplicity in presenting the results and will not affect the analysis.

Smoothing with splines is then applied to the baseline and month-6 activity records so that the resulting PA records in each period are represented by a smooth curve, that is, a smooth function of time of a day. The purpose of this step is to reduce the variability induced by random measurement errors and fluctuations caused by the device, and to increase the signal-to-noise ratio in the activity record to avoid over-fitting in the subsequent analyses. The same smoothing parameters are used for all baseline and month-6 PA records

of all subjects. As discussed in Section 4.1, the smoothing parameter $df = 25$ is selected based on exploratory analysis of both RfH and MENU datasets.

In addition to physical activity records, demographic and medical measurements were collected for each subject in both baseline and month-6 visits. In particular, treatment assignment indicators of medication (metformin and placebo) and life-style intervention (with and without weight-loss program) are available both separately and as a 2×2 factorial design. Other important variables include age, body mass index (BMI), activity minutes at baseline, history of diseases and medication, pathological stage, years from diagnosis, and glucose.

6.2 Estimating Longitudinal Changes in PA

The first step of the estimation is to characterize the longitudinal changes of PA in terms of subject-specific deformations from the baseline activity curves to the month-6 curves. As discussed in Section 3, each subject’s deformation from the baseline curve to the month-6 curve is modeled as a diffeomorphism governed by a vector field, and the vector field is assumed to follow the RKHS representation (4). Moreover, to estimate the deformations, it suffices to estimate the initial momenta $\{m_k\}$ at the control points.

Here we use the function *match_geom()* in the Matlab package *fshapesTK* developed by Charlier et al. (2015b) to estimate the subject-specific initial momenta in deforming the baseline to the month-6 PA curve. Figure 5 shows an example of the estimated deformations. The figure compares the actual month-6 PA curve with the month-6 curve obtained by evolving the baseline curve following the estimated deformation governed by the estimated initial momenta. Middle steps from the baseline to the estimated month-6 curves are also included in the plots. Specifically, the middle steps are curves obtained by mapping the baseline with deformations $\psi_v(\tau, \cdot)$ for $\tau \in (0, 1)$. As described in (1), the deformation at each middle step $\tau \in (0, 1)$ follows the differential equation $\partial\psi_v(\tau, \cdot)/\partial\tau = v_\tau \circ \psi_v(\tau, \cdot)$. In

estimating the momenta, we discretized τ into $\{\tau_k : k = 1, \dots, N_{\text{steps}}\}$ steps and estimated the deformation at each step. The deformed curve at the final step ($k = 11$) is the estimated month-6 curve. Upon examining the discretization we found $N_{\text{steps}} = 11$ steps led to consistently satisfactory approximation of the deformation. For data of much higher dimensionality, exploratory analysis can be conducted to find the appropriate number of steps in the discretization.

As discussed in previous sections, the estimated deformation and initial momenta reveal changes in both PA magnitude and phase. In Figure 5, the estimated initial momenta capture several key characteristics of changes in activity. PA levels decreased throughout the day comparing month 6 to baseline, which is reflected by the downward pointing arrows at most time points. In addition to the decrease in PA magnitudes, there are two visible shifts of active hours: the small peak centered around 9am at baseline visit shifts to the right after six months, while the peak centered around 12pm shifts significantly to the left. The corresponding initial momenta are able to reveal the phase shifts with arrows pointing to the upper right during the 9am peak and to the left during the 12pm peak.

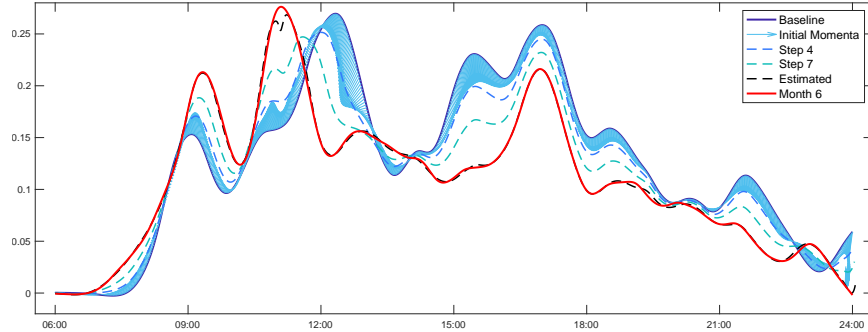


Figure 5: RfH study: estimated deformations. Baseline PA curve (navy) overlapped with estimated initial momenta (visualized by light blue arrows on top of the baseline curve), middle steps of deformations (dashed lines), and estimated (black dashed) and actual month-6 curve (red). y -axis: scaled PA level. x -axis: time of a day.

6.3 fPCA Estimation

The estimated initial momenta of the deformations are concatenated into vectors and the principal components (PCs) of the vectors are extracted from the mean-subtracted momenta. The top 10 PCs explain about 50% of the variance and the top 30 explain over 80% of the variance in the data. See the Supp. Material for the screeplot of variances explained by the top 10 PCs.

In what follows, we will focus on the analysis involving the top 10 PCs. Other PCs that explain less variability in the data may also exhibit interesting patterns of PA change and associations with lifestyle intervention and other covariates. However, since such PCs characterize changes in PA in shorter time windows and are less meaningful and more difficult to interpret, we defer the results to the Supplementary Material.

6.4 Intervention and Covariate Associations With PA Change

We are interested here in the effects of the covariates, the interventions on activity in particular, on different modes of longitudinal changes in PA. To this end we conduct a series of analysis on each of the top 10 PCs. In each separate analysis, the projections (scores) of subject-specific deformations on each PC is the outcome of interest, and lifestyle intervention and relevant demographic and medical variables are the covariates.

Table “RfH Summary Statistics” in the Supplementary Material lists summary statistics of the interventions and other variables. Variables of with more than 5% values missing are discarded for further analysis. Medical conditions with less than 5% missing are imputed with “no” for the missing values.

LASSO regularization with 10-fold cross-validation for the choice of penalty parameter is used to select variables from the covariates. Several variables are discovered as significantly associated with modes of change in PA as characterized by certain PCs. In what follows, we focus on results of PC 1, 4, and 10, which are found to be associated with lifestyle

intervention, in separate subsections. Significant effects of covariates on the corresponding PC projection coefficients are listed, and initial momenta of PCs in question are visualized along with the estimated month-6 curve resulting from deforming the mean baseline curve of all subjects according to the diffeomorphism governed by the initial momenta of the PC. For the purpose of demonstration, we also visualize the month-6 curve resulting from deforming the baseline with the estimated initial momenta of the PC multiplied by -1 to illustrate the opposite direction of the PA change for a subject with negative projection coefficient on the PC. Note each PC can be scaled by a positive or negative constant and still be a well-defined PC as long as the PC scores change are scaled accordingly. For simplicity in interpreting the results, we scale the PCs and corresponding projections/scores so that subjects' projections of each PC have standard deviation equal to one.

6.4.1 PC 1

Figure 6 illustrates the first principal component (PC) via plots of its initial momenta, along with the resulting PA curves from deforming the averaged baseline PA curve following the initial momenta multiplied by $+1$ and -1 . As PC 1 explains most variability in the data, it is not surprising that the mode of change in PA characterized by PC 1 is an overall uplift of activity level (or an overall decrease if one considers -1 times PC 1) from the baseline to month 6. In particular, activity level in the morning from around 8am to 11am increases significantly. The trend of the increase of PA lasts through daytime until around 6pm.

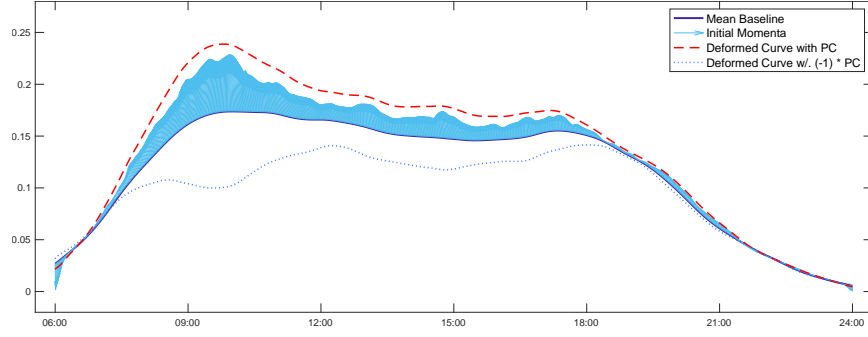


Figure 6: RfH study: estimated deformations of PC 1. Baseline overlaid with estimated initial momenta (arrows on top of the baseline curve) and estimated month-6 curves by applying the deformations corresponding to $+1$ (red) and -1 (dashed blue) multiplying the initial momenta of the PC, respectively.

Life style intervention and medication are not significantly associated with PC 1 projection scores in a two-way analysis of variance (ANOVA). However, in modeling effects on PC 1 while adjusting for other covariates, life-style intervention is selected to be included in the selected model under LASSO regularization. The LASSO penalty parameter is chosen based on a 10-fold cross validation. Table 1 shows the result of a re-run of a separate un-regularized regression analysis using only variables selected by LASSO regularization. Although life-style intervention is not significant in the re-run, its effect is estimated to be positive (0.128) with p -value 0.168, indicating the life-style intervention potentially has a positive effect on promoting daily activity in general.

Covariate	Coef Estimate (SE)	p-value
(Intercept)	2.529 (0.736)	0.001 ***
Life Style Intervention	0.128 (0.092)	0.168
Age	-0.026 (0.007)	0.001 ***
SED	0.002 (0.001)	0.008 **
LPA100	-0.004 (0.001)	<0.001 ***
MVPA1952	-0.020 (0.003)	<0.001 ***
Insomnia: Yes	0.167 (0.103)	0.107
Sleep Disorder: Yes	-0.294 (0.151)	0.053 .
Quality of Life Rating	-0.039 (0.034)	0.253
Diabetes: Yes	0.779 (0.309)	0.012 *
Fracture other than in hip after age 50: Yes	-0.128 (0.123)	0.3
Aspirin: Yes	0.245 (0.110)	0.026 *
Smoke Status: Former	-0.105 (0.093)	0.26
Education completed some high school but did not graduate	-0.834 (0.367)	0.024 *
Education graduated from high school or G.E.D.	0.282 (0.211)	0.183
Education some college	-0.073 (0.126)	0.562
Education postgraduate school or degree, technical school or associate degree	0.170 (0.130)	0.194
Employment on leave of absence	0.432 (0.359)	0.23
Employment disabled and/or retired because of health	-0.395 (0.195)	0.044 *

Table 1: RfH study: coefficient estimates (with standard errors) and p -values of covariates' effects on PC 1 projection scores.

Table 1 also lists estimated effects of LASSO-selected covariates other than the intervention on overall increase in PA as characterized by a positive projection score on PC 1. Cut-point based average minutes categories at baseline: SED (Sedentary Behavior with count per minute CPM < 100), LAP100 (Light Physical Activity with CPM in the range of 100 – 1951), and MVPA1952 (Moderate Vigorous Physical Activity with CPM > 1952) are all significantly correlated with PC 1. For details on above cut-point based categories, see, for example, Amagasa et al. (2018). Signs of the effects associated with the above categories (positive for SED and negative for LAP100 and MVPA1952) are reasonable, as subjects that are less active and more sedentary are expected to have more potential of improvement and thus exhibit an increase in PA during the study.

Age has a significantly negative effect on PC1, indicating older age is associated with less increase in activity over the six-month study period. Subjects with diabetes tend to exhibit increased activity. Given the relatively small number of subjects with diabetes (7

out of 303), however, the effect of diabetes needs to be validated in a more comprehensive analysis of a better balanced dataset. Taking Aspirin (such as Anacin, Bufferin, Bayer, Excedrin) regularly more than three times per week at baseline visit has a positive effect on PC 1. In education categories, completing part of high school but did not graduate has a negative effect on PC 1. Employment status of disabled and/or retired because of health also has a negative effect on PC 1. Although the results are less significant, it is worth noting that having sleep disorder and ever having fractures other than in the hip after age 50 both have negative effects on PC 1 projection scores. Lastly, the randomized assignment of medication (metformin or placebo) is not selected by LASSO.

6.4.2 PC 4

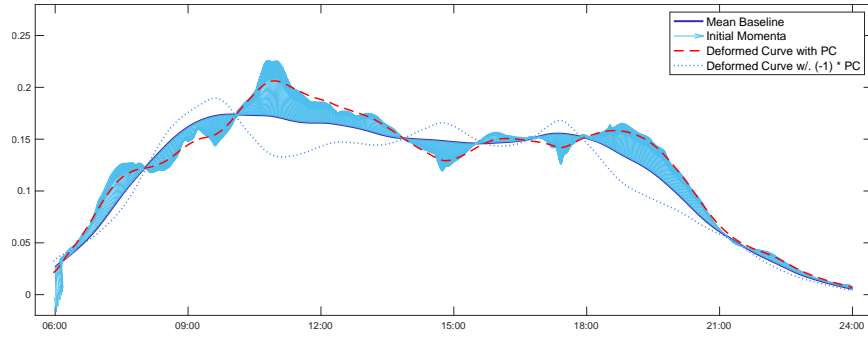


Figure 7: RfH study: estimated deformations of PC 4. Baseline overlaid with estimated initial momenta (arrows on top of the baseline curve) and estimated month-6 curves by applying the deformations corresponding to $+1$ (red) and -1 (dashed blue) multiplying the initial momenta of the PC, respectively.

Figure 7 visualizes the estimated PC 4. The mode of variation in PA given by PC 4 is marked by a significant increase of PA level at mid-day (10am - 1:30pm) and evening (6pm - 9pm). In addition, there is a smaller increase of PA in early morning (6am - 8am) followed by a decrease, indicating a shift of morning activity to early hours. A similar but less manifested shift can be observed from the slight decrease in PA after 1:30pm post the

significant increase during the 10am - 1:30pm period.

Covariate	Coef Estimate (SE)	<i>p</i> -value
(Intercept)	1.381 (0.447)	0.002 **
Life Style Intervention	0.230 (0.113)	0.042 *
LPA100	-0.002 (0.001)	0.011 *
Ever received endocrine treatment	-0.215 (0.140)	0.125
Baseline Weight	-0.007 (0.004)	0.090 .
High Cholesterol: Yes	-0.268 (0.112)	0.017 *
Diabetes: Yes	0.807 (0.376)	0.033 *
Hip Joint Replacement: Yes	-0.231 (0.202)	0.253
Acetaminophen: Yes	-0.201 (0.161)	0.214
Education Graduated from high school or G.E.D.	0.289 (0.236)	0.221
Marital Living with a partner in a marriage like relationship	0.486 (0.298)	0.104
Employment Retired (not due to health)	-0.180 (0.119)	0.131

Table 2: RfH study: coefficient estimates and *p*-values of regression model of PC 4 projection on covariates.

Table 2 summarizes estimated regression coefficients of LASSO-selected covariates in modeling changes of PA in the mode given by PC 4. Life style intervention has a significantly positive effect, indicating subjects in the intervention group are more likely to exhibit a change in PA in the mode of PC 4. Baseline LPA100, weight and high cholesterol all have negative effects on PC 4. Diabetes has a positive effect as in modeling effects on PC 1. Again this result needs to be validated with larger dataset with more subjects having positive diabetes status. Other variables also exhibit effects in expected directions, although less significantly: ever having hip joint replacement, taking acetaminophen (Tylenol) regularly (more than three times per week) and employment status of retired have negative effects on PC 4 projection scores. Again randomized assignment of medication (metformin or placebo) is not selected by LASSO as a relevant predictor.

We also examine the effect of lifestyle intervention on PC 4 via a two-way ANOVA (lifestyle intervention and medication) without adjusting for other covariates. The factor of lifestyle intervention has a mildly significant effect on PC 4 projection scores with *p*-value 0.07 while medication does not have a significant effect.

6.4.3 PC 10

Figure 8 visualizes the estimated PC 10. Changes in PA are generally less manifested throughout the day comparing to previously discussed PCs. The mode of variation characterized by PC 10 is less of an overall increase of PA, but rather a re-distribution of afternoon activities throughout the day and a change of activity habits. Activity levels are increased in the windows of 8am - 9:30am and 10am - 2pm, and decreased between 3pm - 5pm.

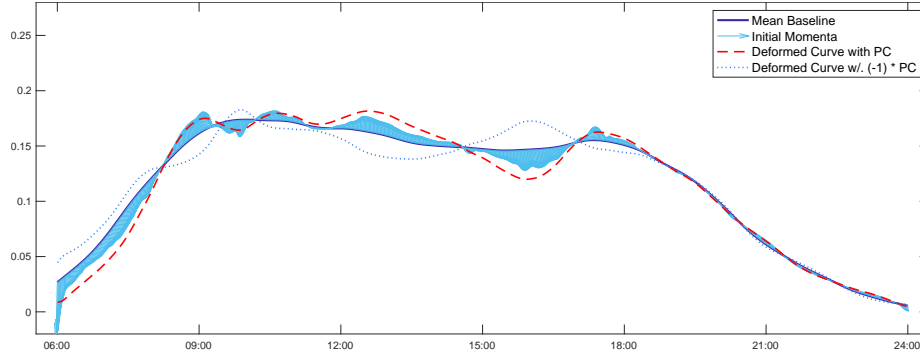


Figure 8: RfH study: estimated deformations of PC 10. Baseline overlaid with estimated initial momenta (arrows on top of the baseline curve) and estimated month-6 curves by applying the deformations corresponding to +1 (red) and -1 (dashed blue) multiplying the initial momenta of the PC, respectively.

Life style intervention has a significantly negative effect on PC 10. This result implies the intervention is associated with, as visualized by the blue dashed curve in Figure 8, a decrease of PA in windows 8am - 9:30am and 10am - 2pm, and an increase between 3pm - 5pm. That is, subjects in the intervention group are more likely to have a migration of morning and early afternoon activities to late afternoon. Glucose value at baseline and fracture other than in the hip after age 50 have negative effects on PC 10, while baseline weight and history of heart disease have positive effects. Employment status of being full time homemaker also has a negative effect on PC 10. Given the low percentage of full time homemaker (13 subjects, 4.3%), this result needs to be further examined in a larger dataset. Randomized assignment of medication (metformin or placebo) is not selected by

LASSO as a relevant predictor. For detailed result for PC 10, see the Supp. Material.

7 Data Analysis II: the MENU Study

The MENU study data consist of 245 overweight non-diabetic women to study the effect of randomly assigned diet interventions on changes in health outcomes in 12 months. Of particular interest is the effect of the interventions on weight loss. In line with this aim, for the analysis of the MENU data, we focus on the role of longitudinal changes in PA on weight loss characterized by changes in BMI.

7.1 Pre-processing of Data

First we pre-process the MENU study data following the same steps as for the RfH data. 184 subjects with both baseline and month-12 PA records available were retained for the analysis after processing. Upon observing the raw PA data, only PA records within the range of 7am to 9pm are kept for the analysis as data out of this range were mostly inactive records. PA records for all subjects are aligned with respect to chronological time of a day. For each subject, the multiple days of measurements are averaged within the same visiting period to reduce noise caused by measurement error and device fluctuation. Smoothing by splines is then applied to the averaged PA records at baseline and month-12 to obtain the PA curves.

7.2 Estimating Longitudinal Changes in PA and fPCA

The same estimation procedure for the subject-specific deformations between the baseline and month-12 PA curves used for the RfH data is applied to the MENU data. fPCA is applied to the estimated initial momenta for each subject's deformation from the baseline PA curve to the month-12 curve. PC 1 explains 10% of the variance, and the top 12 PCs explain over 50%. The top 30 PCs explain over 77% of the variance (see Supp. Material

for screeplot of variance explained).

7.3 Correlative Studies with Health Outcomes

Here we examine the association between discovered modes of changes in PA and health outcomes. The outcome of interest here is the change in BMI, that is, month-12 minus baseline BMI, as an indicator of weight loss during the 12-month study period. We examine models in which change in BMI is the outcome and subjects' projection coefficients on the PCs are the main covariates of interest. Other important covariates including diet interventions are adjusted in the model. Table "MENU Summary Statistics" in the Supplementary Material lists summary statistics of the interventions and other variables.

The analysis consists of two steps. First, we fit a regression with LASSO regularization to select variables including the PCs and other covariates that are associated with the outcome. Second, we fit a separate regression without regularization with only the selected variables.

Covariate	Coef Estimate (SE)	<i>p</i> -value
(Intercept)	-3.655 (1.539)	0.019 *
Education Years	0.137 (0.082)	0.097 .
High cholesterol	1.102 (0.527)	0.038 *
Pain subscale (Quality of Life)	-0.014 (0.009)	0.125
Vigorous activity at work days	0.677 (0.492)	0.170
Weekly Met-Minutes	0.000 (0.000)	0.283
Follicle stimulating hormone	-0.011 (0.005)	0.046 *
PC1	0.752 (0.186)	<0.001 ***
PC5	-0.479 (0.180)	0.008 **
PC13	0.514 (0.179)	0.005 **
PC25	-0.460 (0.187)	0.015 *

Table 3: MENU Study: coefficient estimates and *p*-values in the regression model of changes in BMI on covariates and PCs.

Table 3 lists the result of regression in the second step of analysis, where only variables selected by LASSO regularization are included in the model. PCs 1, 5, 13 and 25 are discovered to be significantly associated with change in BMI. Figures 9 and 10 illustrate the estimated deformations associated with PCs 1 and 5. Plots of PCs 13 and 25 are

deferred to the Supp. Material as those PCs explain less meaningful variance.

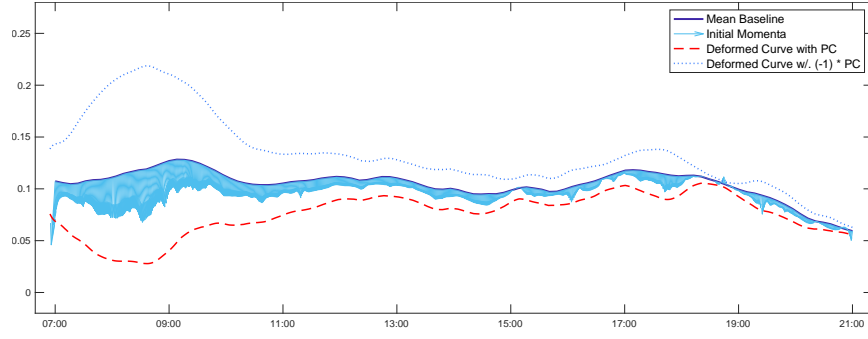


Figure 9: MENU Study: estimated deformations of PC 1.

The red curve in Figure 9 shows that the mode of variation characterized by PC 1 is an overall decrease of activity (or overall elevation if consider PC multiplied by -1 as illustrated by the blue dashed curve). The change of PA is most significant in the morning from 7am - 10am. There is also a decrease in PA of a smaller magnitude from 5pm to 6:30pm. The effect of PC 1 on the change in BMI is positive (0.752 with p -value less than 0.001), indicating a decrease of PA from baseline to month-12 in the mode of PC 1 is associated with an increase of BMI from baseline to month 12. Equivalently, an increase of PA following the pattern of the dashed blue curve is associated with decreased BMI and weight loss.

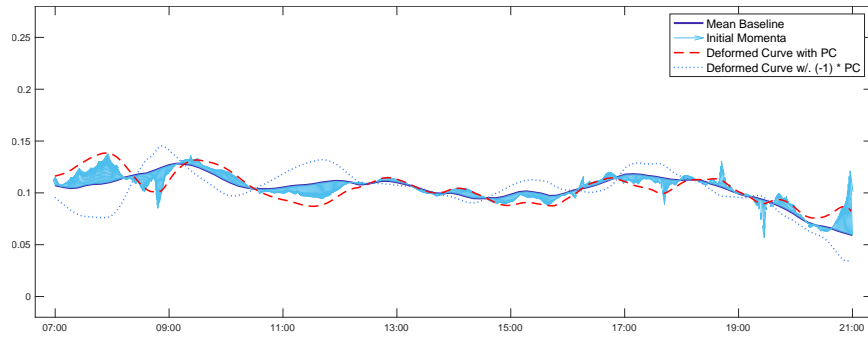


Figure 10: MENU Study: estimated deformations of PC 5.

Figure 10 shows the mode of change in PA given by PC 5. This PC exhibits a re-distribution of morning activity. The PA level is increased in windows 7am - 8:30am and

9:30am - 10:30am and decreased in windows 8:30am - 9:30am and 10:30am - 12pm. The impression is the activity is shifted towards early hours in the morning. The effect of PC 5 on the change in BMI is negative (-0.479 with p -value 0.008), indicating change of PA following the mode of PC 5 is associated with decreased BMI and weight loss.

In addition to the PCs, high cholesterol has a positive effect on weight gain (positive change in BMI) with effect size 1.102 (p -value 0.038) while follicle stimulating hormone (FSH) level has a positive effect with effect size -0.011 (p -value 0.046) on weight loss (negative change in BMI).

8 Concluding Remarks

In this paper we propose a new modeling framework for longitudinal changes in physical activity (PA) and relations between longitudinal changes in PA and health outcomes as well as interventions. The model and method proposed here are based on a Riemann manifold representation of spline-smoothed PA records as functions of chronological time of a day. The longitudinal changes in PA during a multi-month study period are modeled as deformations between PA curves (1D Riemann manifolds) measured in different visiting periods of the study.

The deformations are modeled via diffeomorphisms governed by elements in a reproducing kernel Hilbert space that satisfy minimal-energy constraints. Subject to the constraint, the deformation is determined by the key quantity “initial momenta”, which are vector fields that represent the initial directions and magnitudes to “drag” each point on the baseline curve towards the target curve.

The variability in longitudinal changes of PA within a cohort of subjects is modeled through the variability of the deformations. Specifically, we adopt the functional principal component analysis (fPCA) to model the variability in subject-specific initial momenta.

We focus on top principal components (PC) that are capable of explaining most of the variability in the cohort and examine the corresponding modes of variation in longitudinal changes in PA. In studying the longitudinal changes in PA of the subjects, of interest are the projection coefficients on the PCs for each subject, which characterize the composition of difference modes of changes in PA for each subject.

In modeling the relations between changes in PA and health outcomes/interventions, subjects' projection coefficients on PCs are used as the proxy for longitudinal changes in PA and are linked to the outcomes/interventions. We apply the proposed model and method to data from two clinical trials: RfH and MENU. For the RfH we use a linear model to examine the effect of the lifestyle intervention on projections on the top PCs while adjusting for relevant covariates selected by LASSO regularization. Several top PCs characterizing different modes of changes in PA are discovered to be significantly associated with the intervention. For the MENU study we use a regression model to study the effect of different modes of changes in PA, as characterized by the top PCs, on the change in BMI while adjusting for relevant covariates selected by LASSO regularization. Several top PCs are significantly associated with change in BMI, indicating corresponding modes of changes in activity habits and patterns are potentially beneficial in achieving weight loss.

Models considered here can be readily generalized to study a variety of problems involving longitudinal changes in physical activity. For example, the effect of PA can be examined in a mediation analysis where the PC projections are potential mediators on the pathway from diet/lifestyle intervention to health outcomes. The PCs can also be studied in machine learning models to predict health outcomes.

Comparing to existing methods relying on summary statistics, the proposed model and method enable new activity patterns to be recognized and important information to be revealed from activity tracker data. As demonstrated in our data analysis, extra information can be revealed about changes in PA and their relationship with health outcomes and

interventions. In particular, boost of activity in certain time windows and/or shifts of active hours to certain periods are found to be associated with lifestyle intervention and can be more effective in facilitating weight loss. Subjects with certain characteristics may have higher tendencies to experience changes in PA in certain modes. This kind of information is valuable in advising and treating patients, and in designing individualized programs according to subject’s personal medical history and conditions.

In future studies, we will explore details in modeling PA records collected from more than two visits. In addition, we are interested in further methodology development for statistical inference on changes in PA characterized by deformations of PA curves. For example, functional regression approaches can be adapted to study effects of covariates on longitudinal changes in PA and/or effect of PA changes on health outcomes. The initial momenta, which are key quantities in modeling deformations of PA curves, can also be modeled as two-dimensional random fields and it is of interest to study their theoretical properties and implications for inference in correlative studies.

References

- Adamo, K. B., Prince, S. A., Tricco, A. C., Connor Gorber, S., and Tremblay, M. (2009). A comparison of indirect versus direct measures for assessing physical activity in the pediatric population: A systematic review. *International Journal of Pediatric Obesity*, 4(1):2–27.
- Ainsworth, B., Cahalin, L., Buman, M., and Ross, R. (2014). The Current State of Physical Activity Assessment Tools. *Progress in Cardiovascular Diseases*, 57(4):387–395.
- Amagasa, S., Machida, M., Fukushima, N., Kikuchi, H., Takamiya, T., Odagiri, Y., and Inoue, S. (2018). Is objectively measured light-intensity physical activity associated with health outcomes after adjustment for moderate-to-vigorous physical activity in adults? A systematic review. *International Journal of Behavioral Nutrition and Physical Activity*, 15(1):1–13.
- Bassett, D. R. (2012). Device-based monitoring in physical activity and public health research. *Physiological Measurement*, 33(11):1769–1783.
- Beg, M. F., Miller, M. I., Trounev, A., and Younes, L. (2005). Computing Large Deformation Metric Mappings via Geodesic Flows of Diffeomorphisms. *International Journal of Computer Vision*, 61(2):139–157.

- Bellettiere, J., LaMonte, M. J., Unkart, J., Liles, S., Patel, D. L., Manson, J. E., Banack, H., Fowler, R. S., Chavez, P., Tinker, L. F., Wallace, R. B., and LaCroix, A. Z. (2020). Short Physical Performance Battery and Incident Cardiovascular Events Among Older Women. *Journal of the American Heart Association*.
- Bijnen, F. C., Caspersen, C. J., and Mosterd, W. L. (1994). Physical inactivity as a risk factor for coronary heart disease: a WHO and International Society and Federation of Cardiology position statement. *Bulletin of the World Health Organization*, 72(1):1–4.
- Blair, S. N. (2009). Physical inactivity: the biggest public health problem of the 21st century. *British Journal of Sports Medicine*, 43(1):1–2.
- Charlier, B., Charon, N., and Trouvé, A. (2015a). The Fshape Framework for the Variability Analysis of Functional Shapes. *Foundations of Computational Mathematics*, 17(2):287–357.
- Charlier, B., Charon, N., and Trouvé, A. (2015b). The Fshape Framework for the Variability Analysis of Functional Shapes. *Foundations of Computational Mathematics*, 17(2):287–357.
- Chastin, S. F. M., De Craemer, M., De Cocker, K., Powell, L., Van Cauwenberg, J., Dall, P., Hamer, M., and Stamatakis, E. (2019). How does light-intensity physical activity associate with adult cardiometabolic health and mortality? Systematic review with meta-analysis of experimental and observational studies. *British Journal of Sports Medicine*, 53(6):370–376.
- Colley, R. C., Garrigué, D., Janssen, I., Craig, C. L., Clarke, J., and Tremblay, M. S. (2011). Physical activity of Canadian adults: accelerometer results from the 2007 to 2009 Canadian Health Measures Survey. *Health reports*, 22(1):7–14.
- Di, C.-Z., Crainiceanu, C. M., Caffo, B. S., and Punjabi, N. M. (2009). Multilevel Functional Principal Component Analysis. *The Annals of Applied Statistics*, 3(1):458–488.
- Dyrstad, S. M., Hansen, B. H., Holme, I. M., and Anderssen, S. A. (2014). Comparison of Self-reported versus Accelerometer-Measured Physical Activity. *Medicine & Science in Sports & Exercise*, 46(1):99–106.
- Ekelund, U., Tarp, J., Steene-Johannessen, J., Hansen, B. H., Jefferis, B., Fagerland, M. W., Whincup, P., Diaz, K. M., Hooker, S. P., Chernofsky, A., Larson, M. G., Spartano, N., Vasan, R. S., Dohrn, I.-M., Hagströmer, M., Edwardson, C., Yates, T., Shiroma, E., Anderssen, S. A., and Lee, I.-M. (2019). Dose-response associations between accelerometry measured physical activity and sedentary time and all cause mortality: systematic review and harmonised meta-analysis. *BMJ*, 366:l4570.
- Füzéki, E., Engeroff, T., and Banzer, W. (2017). Health Benefits of Light-Intensity Physical Activity: A Systematic Review of Accelerometer Data of the National Health and Nutrition Examination Survey (NHANES). *Sports Medicine*, 47(9):1769–1793.
- Goldsmith, J., LIU, X., JACOBSON, J. S., and RUNDLE, A. (2016). New Insights into Activity Patterns in Children, Found Using Functional Data Analyses. *Medicine & Science in Sports & Exercise*, 48(9):1723–1729.

- Goldsmith, J., Zipunnikov, V., and Schrack, J. (2015). Generalized multilevel function-on-scalar regression and principal component analysis. *Biometrics. Journal of the International Biometric Society*, 71(2):344–353.
- Greven, S., Crainiceanu, C., Caffo, B., and Reich, D. (2010). Longitudinal functional principal component analysis. *Electronic Journal of Statistics*, 4(none):1022–1054.
- Greven, S., Crainiceanu, C., Caffo, B., and Reich, D. (2011). Longitudinal Functional Principal Component Analysis. In *Recent Advances in Functional Data Analysis and Related Topics*, pages 149–154. Physica-Verlag HD.
- Hernandez, M., Bossa, M. N., and Olmos, S. (2009). Registration of Anatomical Images Using Paths of Diffeomorphisms Parameterized with Stationary Vector Field Flows. *International Journal of Computer Vision*, 85(3):291–306.
- Khan, K. M. and Scott, A. (2009). Mechanotherapy: how physical therapists’ prescription of exercise promotes tissue repair. *British Journal of Sports Medicine*, 43(4):247–252.
- Khan, W. A. A., Jackson, M. L., Kennedy, G. A., and Conduit, R. (2021). A field investigation of the relationship between rotating shifts, sleep, mental health and physical activity of Australian paramedics. *Scientific Reports*, 11(1):1–11.
- Knoops, K. T. B., de Groot, L. C. P. G. M., Kromhout, D., Perrin, A.-E., Moreiras-Varela, O., Menotti, A., and van Staveren, W. A. (2004). Mediterranean diet, lifestyle factors, and 10-year mortality in elderly European men and women: the HALE project. *JAMA*, 292(12):1433–1439.
- Kohl, H. W. (2001). Physical activity and cardiovascular disease: evidence for a dose response. *Medicine & Science in Sports & Exercise*, 33(6 Suppl):S472–83– discussion S493–4.
- LaCroix, A. Z., Bellettiere, J., Rillamas-Sun, E., Di, C., Evenson, K. R., Lewis, C. E., Buchner, D. M., Stefanick, M. L., Lee, I.-M., Rosenberg, D. E., LaMonte, M. J., and WHI, f. t. W. H. I. (2019). Association of Light Physical Activity Measured by Accelerometry and Incidence of Coronary Heart Disease and Cardiovascular Disease in Older Women. *JAMA Network Open*, 2(3):e190419–e190419.
- LaMonte, M. J., Buchner, D. M., Rillamas-Sun, E., Di, C., Evenson, K. R., Bellettiere, J., Lewis, C. E., Lee, I.-M., Tinker, L. F., Seguin, R., Zaslovsky, O., Eaton, C. B., Stefanick, M. L., and LaCroix, A. Z. (2018). Accelerometer-Measured Physical Activity and Mortality in Women Aged 63 to 99. *Journal of the American Geriatrics Society*, 66(5):886–894.
- Le, T., Flatt, S. W., Natarajan, L., Pakiz, B., Quintana, E. L., Heath, D. D., Rana, B. K., and Rock, C. L. (2016). Effects of Diet Composition and Insulin Resistance Status on Plasma Lipid Levels in a Weight Loss Intervention in Women. *Journal of the American Heart Association*.
- Li, H., Kozey Keadle, S., Staudenmayer, J., Assaad, H., Huang, J. Z., and Carroll, R. J. (2015). Methods to assess an exercise intervention trial based on 3-level functional data. *Biostatistics*, 16(4):754–771.

- Li, H., Staudenmayer, J., and Carroll, R. J. (2014). Hierarchical functional data with mixed continuous and binary measurements. *Biometrics. Journal of the International Biometric Society*, 70(4):802–811.
- Loprinzi, P. D. (2016). Light-Intensity Physical Activity and All-Cause Mortality. *American Journal of Health Promotion*, 31(4):340–342.
- Matthews, C. E., Ockene, I. S., Freedson, P. S., Rosal, M. C., Merriam, P. A., and Hebert, J. R. (2002). Moderate to vigorous physical activity and risk of upper-respiratory tract infection. *Medicine & Science in Sports & Exercise*, 34(8):1242–1248.
- Miguelles, J. H., Cadenas-Sanchez, C., Ekelund, U., Nyström, C. D., Mora-Gonzalez, J., Löf, M., Labayen, I., Ruiz, J. R., and Ortega, F. B. (2017). Accelerometer Data Collection and Processing Criteria to Assess Physical Activity and Other Outcomes: A Systematic Review and Practical Considerations. *Sports Medicine*, 47(9):1821–1845.
- Montaruli, A., Galasso, L., Caumo, A., Cè, E., Pesenti, C., Roveda, E., and Esposito, F. (2017). The circadian typology: the role of physical activity and melatonin. *Sport Sciences for Health*, 13(3):469–476.
- Nader, P. R., Bradley, R. H., Houts, R. M., McRitchie, S. L., and O’Brien, M. (2008). Moderate-to-vigorous physical activity from ages 9 to 15 years. *JAMA*, 300(3):295–305.
- Parada, H., McDonald, E., Bellettiere, J., Evenson, K. R., LaMonte, M. J., and LaCroix, A. Z. (2020). Associations of accelerometer-measured physical activity and physical activity-related cancer incidence in older women: results from the WHI OPACH Study. *British Journal of Cancer*, 122(9):1409–1416.
- Patterson, R. E., Marinac, C. R., Natarajan, L., Hartman, S. J., Cadmus-Bertram, L., Flatt, S. W., Li, H., Parker, B., Oratowski-Coleman, J., Villaseñor, A., Godbole, S., and Kerr, J. (2016). Recruitment strategies, design, and participant characteristics in a trial of weight-loss and metformin in breast cancer survivors. *Contemporary clinical trials*, 47:64–71.
- Patterson, R. E., Marinac, C. R., Sears, D. D., Kerr, J., Hartman, S. J., Cadmus-Bertram, L., Villaseñor, A., Flatt, S. W., Godbole, S., Li, H., Laughlin, G. A., Oratowski-Coleman, J., Parker, B. A., and Natarajan, L. (2018). The Effects of Metformin and Weight Loss on Biomarkers Associated With Breast Cancer Outcomes. *J Natl Cancer Inst*, 110(11):1239–1247.
- Prince, S. A., Adamo, K. B., Hamel, M., Hardt, J., Connor Gorber, S., and Tremblay, M. (2008). A comparison of direct versus self-report measures for assessing physical activity in adults: a systematic review. *International Journal of Behavioral Nutrition and Physical Activity*, 5(1):56–24.
- Reuter, C., Bellettiere, J., Liles, S., Di, C., Sears, D. D., LaMonte, M. J., Stefanick, M. L., LaCroix, A. Z., and Natarajan, L. (2020). Diurnal patterns of sedentary behavior and changes in physical function over time among older women: a prospective cohort study. pages 1–11.
- Rock, C. L., Flatt, S. W., Pakiz, B., Quintana, E. L., Heath, D. D., Rana, B. K., and Natarajan, L. (2016). Effects of diet composition on weight loss, metabolic factors and biomarkers in a 1-year weight loss intervention in obese women examined by baseline insulin resistance status. *Metabolism: clinical and experimental*, 65(11):1605–1613.

- Shou, H., Zipunnikov, V., Crainiceanu, C. M., and Greven, S. (2014). Structured functional principal component analysis. *Biometrics. Journal of the International Biometric Society*, 71(1):247–257.
- Stamatakis, E., Gale, J., Bauman, A., Ekelund, U., Hamer, M., and Ding, D. (2019). Sitting Time, Physical Activity, and Risk of Mortality in Adults. *Journal of the American College of Cardiology*.
- Sullivan, P. W., Morrato, E. H., Ghushchyan, V., Wyatt, H. R., and Hill, J. O. (2005). Obesity, inactivity, and the prevalence of diabetes and diabetes-related cardiovascular comorbidities in the U.S., 2000-2002. *Diabetes care*, 28(7):1599–1603.
- Vaillant, M., Miller, M. I., Younes, L., and Trouvé, A. (2004). Statistics on diffeomorphisms via tangent space representations. *Neuroimage*, 23(1):S161–S169.
- Wilmot, E. G., Edwardson, C. L., Achana, F. A., Davies, M. J., Gorely, T., Gray, L. J., Khunti, K., Yates, T., and Biddle, S. J. H. (2012). Sedentary time in adults and the association with diabetes, cardiovascular disease and death: systematic review and meta-analysis. *Diabetologia*, 55(11):2895–2905.
- Xiao, L., Huang, L., Schrack, J. A., Ferrucci, L., Zipunnikov, V., and Crainiceanu, C. M. (2015). Quantifying the lifetime circadian rhythm of physical activity: a covariate-dependent functional approach. *Biostatistics*, 16(2):352–367.
- Xu, S. Y., Nelson, S., Kerr, J., Godbole, S., Johnson, E., Patterson, R. E., Rock, C. L., Sears, D. D., Abramson, I., and Natarajan, L. (2019). Modeling Temporal Variation in Physical Activity Using Functional Principal Components Analysis. *Statistics in Biosciences*, 11(2):403–421.